THE JOURNAL OF PHYSICAL CHEMISTRY B

Article

pubs.acs.org/JPCB

Thermal Stability of Hydrophobic Helical Oligomers: A Lattice Simulation Study in Explicit Water

Santiago Romero-Vargas Castrillón,*[,†] Silvina Matysiak,[‡] Frank H. Stillinger,[§] Peter J. Rossky,[∥] and Pablo G. Debenedetti[†]

[†]Department of Chemical and Biological Engineering, Princeton University, Princeton, New Jersey 08544, United States

[‡]Fischell Department of Bioengineering, University of Maryland, College Park, Maryland 20742, United States

[§]Department of Chemistry, Princeton University, Princeton, New Jersey 08544, United States

[∥]Institute for Computational Engineering and Sciences and Department of Chemistry and Biochemistry, University of Texas at Austin, Austin, Texas 78712, United States

ABSTRACT: We investigate the thermal stability of helical hydrophobic oligomers using a three-dimensional, water-explicit lattice model and the Wang–Landau Monte Carlo method. The degree of oligomer helicity is controlled by the parameter $\varepsilon_{mm} < 0$, which mimics monomer–monomer hydrogen bond interactions leading to the formation of helical turns in atomistic proteins. We vary $|\varepsilon_{mm}|$ between 0 and 4.5 kcal/mol and therefore investigate systems ranging from flexible homopolymers (i.e., those with no secondary structure) to helical oligomers that are stable over a broad range of temperatures. We find that systems with $|\varepsilon_{mm}| \leq 2.0$ kcal/mol exhibit a broad thermal unfolding transition at high temperature, leading to an ensemble of random coils. In contrast, the structure of conformations involved in a second, low-temperature, transition is strongly dependent on $|\varepsilon_{mm}|$. Weakly helical oligomers are observed when $|\varepsilon_{mm}| \leq 1.0$ kcal/mol and exhibit a low-temperature, cold-unfolding-like transition to an ensemble of strongly water-penetrated globular conformations. For higher $|\varepsilon_{mm}|$ (1.7 kcal/mol $\leq |\varepsilon_{mm}| \leq$ 2.0 kcal/mol), cold unfolding is suppressed, and the low-temperature conformational transition becomes a "crystallization", in which a "molten" helix is transformed into a defect-free helix. The molten helix preserves ≥50% of the helical contacts observed in the "crystal" at a lower temperature. When $|\varepsilon_{mm}| = 4.5$ kcal/mol, we find that conformational transitions are largely suppressed within the range of temperatures investigated.

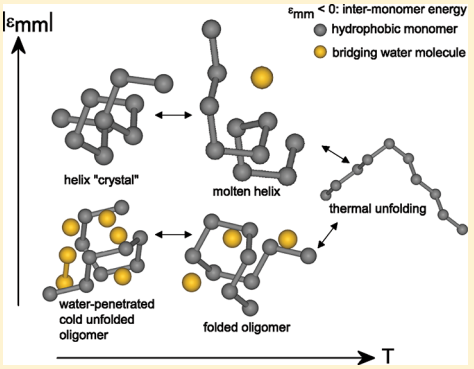

1. INTRODUCTION

It is well established that hydrophobic interactions—the tendency of apolar solutes to aggregate in aqueous solution—represent the principal contribution to the free energy of protein folding.[1−3] Their importance was first proposed by Kauzmann,[2] who noted that protein thermal stability (i.e., the temperature dependence of the free energy of unfolding) follows the same nonmonotonic behavior as the free energy of transfer of hydrocarbons from nonaqueous into aqueous media. The hydrophobic effect thus explains why proteins adopt their active conformation only within a narrow temperature range, undergoing denaturation upon heating or cooling (mirroring the increase in hydrocarbon solubility in water at low or high temperature). That this model, derived from systems as simple as aqueous hydrocarbons, successfully explains the stability of molecules as complex as proteins is truly remarkable.[3,4] However, hydrophobic interactions, being highly nonspecific, are unable to fully explain the folding event, falling short of prescribing the formation of protein secondary structure.[1] The latter, comprised of helices and sheets,[1] arises from the addition of electrostatic interactions, disulfide bridges, and hydrogen bonds (HBs), which are directional interactions between specific backbone and side-chain groups. The hydrocarbon model of protein folding[2] is thus completed by considering that there is a concerted effect of both hydrophobic interactions, which fold the amino acid chain into a compact globule with a relatively dry core, and directional interactions such as hydrogen bonding, which lead to structural specificity. The latter, though apparently of secondary importance in the overall folding thermodynamics, is responsible for the fine internal architecture of native protein structures.[1]

Recent statistical-mechanical lattice models[5,6] have shown that, by explicit treatment of the solvent and the thermodynamics of hydrophobic solvation, it is possible to capture the main features of the conformational phase diagram of a protein-like, hydrophobic oligomer:[6,7] these include water-penetrated, cold-unfolded states at low temperature (T); an ensemble of disordered, compact states at intermediate T; and thermally denatured conformations at high T.[7] This behavior, however, will be altered by the inclusion of intermonomer interactions

Received: May 26, 2012
Revised: July 15, 2012
Published: August 10, 2012

   dx.doi.org/10.1021/jp305134w | J. Phys. Chem. B 2012, 116, 9963–9970

that result in protein secondary structure, giving rise to structurally different oligomer conformations, and even the suppression of temperature-driven conformational transitions, such as the observed disappearance of cold denaturation in largely α-helical peptides.[8]

In this paper we show that a minimalist lattice model, incorporating hydrophobicity and meaningful intermonomer energetics, suffices to investigate the temperature-driven conformational transitions of oligomers possessing secondary structure. Specifically, we systematically study the effect of intermonomer interaction strength on the thermal stability of a solvated hydrophobic decamer, focusing on interactions leading to the formation of helical turns. Our results show that, upon increasing the strength of helix-promoting monomer−monomer interactions, the low-T decamer conformation evolves from a cold-denatured ensemble to one composed of polymers with >95% helical content (as determined from the number of helical contacts). At intermediate T, with increasing $|\varepsilon_{mm}|$, the oligomer conformations evolve from a disordered, compact globule, to an extended helical conformation.

This paper is structured as follows. In sections 2 and 3 we present the lattice model and discuss the simulation technique and data analysis protocol. The simulation results are presented in section 4, followed by discussion in section 5 and a summary of the main conclusions in section 6.

2. LATTICE MODEL

We study the thermal stability of helical oligomers by considering a lattice representation of a hydrophobic polymer in explicit water. As in previous work,[6] the solvated oligomer is mapped onto a body-centered cubic (bcc) lattice, a geometry compatible with the formation of helical contacts.[9,10] A bcc lattice can be conceived as two interpenetrating tetrahedral lattices,[11] with each site (which may be empty or occupied by a water molecule or monomer) having 8 nearest neighbors (*nn*) placed at a distance $3^{1/2}$. Virtual bonds, represented by relative coordinate alternatives $[\pm1, \pm1, \pm1]$, join *nn* sites. Multiple site occupancy is forbidden. A modified form of the lattice model by Roberts and Debenedetti[12] is chosen as a model of the water-like solvent. Water molecules have four bonding arms in a tetrahedral arrangement, each of which may point to a *nn* site. Molecular orientations are discretized by a Potts variable, $\sigma_i = 1, ..., q$; q is the number of distinguishable orientations. Hydrogen bonding occurs between *nn* molecules with favorably oriented bonding arms (*vide infra*). Alternatively, *nn* molecules with misaligned bonding arms can engage in nondirectional, van der Waals-like interactions. HB and van der Waals interaction energies were parametrized using molecular dynamics simulations of a hydrophobic oligomer in explicit water.[13] The occurrence of stronger HBs when density is locally low,[14,15] and the observation that the van der Waals interactions are weakened by the presence of *nn* molecules[13] is incorporated into the model by making the corresponding interaction energies (ε_{HB} and ε_{vdW}, respectively) dependent on the number of nearest neighbors, N_{nn}. We note that the solvent model[6] differs from the original formulation by Roberts and Debenedetti[12] in that ε_{vdW} is also a function of N_{nn}. Information on the parametrization of water−water interactions may be found elsewhere.[13]

MD simulations and spectroscopic studies[16−18] have shown that water molecules participating in hydrophobic solvation exhibit slower dynamics relative to the bulk liquid, and a preferential orientation in which HB arms are tangential to the solute or residue, allowing water molecules to preserve, as much as possible, their HB connectivity.[13,16,19] Consequently, water molecules participating in hydrophobic hydration exist in a set of restricted configurations with a lower entropy. Moreover, given the fact that molecules participating in hydrophobic hydration form more directional hydrogen bonds owing to their reduced rotational entropy, the HB energy between two such molecules is stronger (more negative).[16,20] Conversely, bulk water molecules are undeterred by the hydrophobe and the bulk has a higher entropy at the expense of more distorted (hence, weaker) HBs. These aspects of the configurational entropy are incorporated into the model[6] following the work of Patel et al.,[5] by distinguishing between the formation of HBs in the bulk vis-á-vis those in which at least one molecule is within the hydrophobic hydration layer. To allow for the broader range of orientations conducive to bulk HBs, an orientational mismatch λ_b is allowed for bulk molecules. Consequently, a bulk−bulk HB exists if the orientations of molecules i and j satisfy $|\sigma_i - \sigma_j| \leq \lambda_b$. As in previous work,[6] we take $\lambda_b = 1$. On the contrary, pairs in which at least one water molecule is in the hydration layer (i.e., *nn* to a monomer) are required to have exactly matching orientations; for hydration HBs, the more stringent requirement $\sigma_i = \sigma_j$ applies. The stronger HBs in the hydration layer are accounted for by adding an energetic bonus to the HB energy, which results in the interaction energy $\varepsilon''_{HB}(N_{nn}) = \varepsilon_{HB}(N_{nn}) + \varepsilon_{HB}^{\text{bonus}}$ for hydration layer HBs. The value of the enthalpic bonus, $\varepsilon_{HB}^{\text{bonus}} = -0.2$ kcal/mol, was also determined from MD simulations of a hydrophobic oligomer in explicit water.[13] For compact notation, we define $\varepsilon''_{HB}(N_{nn}) = \varepsilon_{HB}(N_{nn})$ for bulk water molecules.

The above considerations lead to the following Hamiltonian for water−water interactions:

$$\mathcal{H}_{ww} = \frac{1}{2}\sum_{\langle i,j\rangle} nw_i nw_j[\gamma_{\sigma_i\sigma_j}\varepsilon''_{HB}(N_{nn}) + (1 - \gamma_{\sigma_i\sigma_j})\varepsilon_{vdW}(N_{nn})] \quad (1)$$

where the occupation variable nw_i is equal to 1 if site i is occupied by a water molecule and zero otherwise; $\gamma_{\sigma_i\sigma_j} = 1$ if molecules i and j have bonding arms aligned for H-bonding (i.e., $\sigma_i = \sigma_j$ if i and/or j are in the hydration layer, or $|\sigma_i - \sigma_j| \leq \lambda_b$ if bulk). The summation runs over nearest-neighbor sites.

The oligomer is modeled as a self-avoiding walk on one of the tetrahedral lattices that underlie the bcc lattice. Sites occupied by a monomer constitute an α-carbon representation of an amino acid residue.[9,10] Consequently, an N_m-mer consists of N_m consecutive sites joined by $N_m - 1$ bonds, where bond lengths and angles are fixed to $3^{1/2}$ and $\cos^{-1}(-1/3) \approx 109.5°$, respectively. The three-dimensional lattice allows the existence of three distinguishable polymer rotational conformations defined by every four monomers: the in-plane trans, with a 180° torsional angle; and two out-of-plane conformations, gauche+ and gauche−, with torsional angles of +60° and −60°, respectively. The oligomer Hamiltonian is inspired by the early Monte Carlo simulations by Skolnick and collaborators,[9,10,21] who studied a family of implicit-water lattice models capable of generating α-helical and β-sheet structural motifs. Drawing from these studies, Matysiak et al.[6] recently studied the temperature stability of a β-hairpin using a 3-D lattice model in explicit water. Here, we build upon this work and study the temperature stability of a helical decamer using a 3-D, water-explicit lattice model. Following the work of Sikorski and Skolnick,[9,10] we consider a Hamiltonian in which monomer−

dx.doi.org/10.1021/jp305134w | J. Phys. Chem. B 2012, 116, 9963−9970

monomer interactions favor the formation of helical contacts. More specifically, a helix stabilization energy, $\varepsilon_{mm} < 0$, is added whenever a left-handed helical turn, produced by two consecutive gauche− conformations, occurs along the polymer. This stabilization (or α_L-helical bias) mimics the HB between the carboxyl O atom of one residue and the amino H atom of an amino acid separated in the sequence by 4 on the chain of an atomistic protein.[22] To formalize this, the oligomer contribution to the potential energy is described by the Hamiltonian

$$\mathcal{H}_{mm} = \frac{1}{2}\sum_{i=1}^{N_m}\sum_{|j-i|=4}\delta_{r_{ij},4} f_{g-}^{i,j}\varepsilon_{mm} \tag{2}$$

In eq 2, $\delta_{r_{ij},4}$ is equal to 1 when the distance between residues i and j is 4, corresponding to the spacing between the i and $i + 4$ residues in a lattice helical turn; N_m is the length of the oligomer chain (10 in this work), and f_{g-}^{ij} is given by

$$f_{g-}^{i,j} = \begin{cases} 1 & \text{if } i \text{ and } j \text{ are in gauche− states} \\ 0 & \text{otherwise} \end{cases}$$

We recall that, in addition to monomer−monomer helical interactions, excluded-volume monomer−monomer interactions forbidding multiple occupancy of a lattice site are accounted for. In this work, our goal is to determine whether a minimalist model that includes only hydrophobicity and intraprotein energetics suffices to describe the thermal response of helical oligomers. Hence, the additional effect of water−monomer interactions beyond excluded volume has not been studied. Hence, the total potential energy of the oligomer−water system is given by

$$\mathcal{H}_{\text{total}} = \mathcal{H}_{ww} + \mathcal{H}_{mm} \tag{3}$$

3. SIMULATION METHOD

The oligomer−water lattice model is studied using the Wang−Landau (WL) algorithm.[23,24] Since the WL technique yields the density of states of a system, it is, in principle, possible to investigate a wide range of temperature conditions from a single simulation, given that T—the absolute temperature—becomes a parameter (*vide infra*). Further, WL is an effective route to study the low-temperature behavior of a solvated polymer, a condition under which the Metropolis Monte Carlo (MC) method is inefficient.[7,23,25] By performing a random walk in energy space, WL overcomes the potential for trapping in local minima that can arise in a MC simulation at constant temperature, and WL is therefore ideal for the investigation of, e.g., protein conformational transitions, particularly cold unfolding. The WL method and its implementation, which we summarize next, have been presented in detail elsewhere.[6,7,23,24] The essence of the algorithm is a random walk over a range of attainable energy levels; the transition probability is proportional to $1/\Omega$, where Ω is the density of states (DOS). Initially, $\Omega(E) = 1$ for all energy levels E. For computational efficiency, the energy range is subdivided into a series of overlapping subranges or "windows", each run in a separate processor.[6] The simulation then proceeds via attempting MC-type moves involving the oligomer and water molecules,[7] with an acceptance probability given by

$$p(E_o \to E_n) = \min\left[1, \frac{\Omega(E_o)}{\Omega(E_n)}\right] \tag{4}$$

where the subscripts o and n denote the old and new configurations, respectively. Whenever an energy state is visited, the DOS is updated according to $\Omega(E) \to \Omega(E)f$, where f is a modification factor (initialized to $f_0 = e \approx 2.718\,28$). In addition, a histogram H is updated every time an energy state is visited, i.e., $H(E) \to H(E) + 1$. The updates on Ω and H are performed using the old energy state E_o after move rejection or with the new state E_n after acceptance. The random walk in energy continues at fixed f until all energy states are visited a sufficient number of times, i.e., here, when $H(E) \geq H_{\min} = 100$. Upon meeting this criterion for histogram flatness, the modification factor is decreased according to the recursion $f_{i+1} = f_i^{1/2}$, the energy histogram is reset to zero (but not the DOS), and a new random walk in energy space begins with the refined modification factor. The algorithm is repeated until f approaches unity to within some tolerance, typically set to $\sim 1 \times 10^{-6}$.

3.1. Simulation Details and Data Analysis. We study systems in which a hydrophobic decamer is solvated in $N = 291$ water molecules. This results in a water fractional density ($\rho_f = N/B$, where $B = 432$ is the total number of lattice sites) of 0.67. This fractional density yields for pure water an interaction energy per molecule and a distribution of N_{nn} around a H-bonded pair close to those identified from MD simulations of water under physiological conditions (−14.5 kcal/mol and ∼5 *nn*, respectively).[6,13] As in previous work,[7] the number of distinguishable water molecule orientations is set to $q = 84$, a value chosen on practical grounds. Even this value results in a required CPU time of up to CPU years to sample the complete energy range ($E_{\min} \approx -2600$ kcal/mol). For economical reasons, and given that we find that the chosen value suffices to observe the conformational transitions that are the objective of this work, higher q values have not been explored. To elucidate the temperature dependence of the oligomer conformations, we conducted simulations over a broad range of the helical stabilization energy ε_{mm}, from 0 kcal/mol—in which case the oligomer Hamiltonian lacks any structural bias, and behaves as a flexible homopolymer[7]—to −4.5 kcal/mol, a typical optimal hydrogen bond interaction energy. The data analysis protocol is analogous to that previously reported.[6,7] With the determined DOS we performed WL simulations with fixed transition rates in order to calculate a series of structural properties. At each condition of $|\varepsilon_{mm}|$, at least 2 (and, typically, 10) statistically independent analysis simulations are run to compute the structural properties. The outcome of the analysis simulations is a series of observables, $\overline{O(E)}$, each of which is reweighted in the canonical ensemble to obtain its temperature dependence

$$\langle O(T)\rangle = \frac{\sum_E \overline{O(E)}\Omega(E)\exp(-\beta E)}{\sum_E \Omega(E)\exp(-\beta E)} \tag{5}$$

where $\beta = 1/k_B T$ and k_B is Boltzmann's constant.

We investigated the temperature dependence of various oligomer structural properties including the radius of gyration, $\langle R_g\rangle$, given by

$$R_g = \left(\frac{1}{2N_m^{\,2}}\sum_i\sum_j |\mathbf{r}_i - \mathbf{r}_j|^2\right)^{1/2} \tag{6}$$

where $\mathbf{r}_i$ is the position vector of monomer i. To characterize oligomer solvation, we computed the number of hydration-layer water molecules (i.e., those molecules adjacent to 1 or more monomers), $\langle N_{Hyd}\rangle$, and the number of monomer−

dx.doi.org/10.1021/jp305134w | J. Phys. Chem. B 2012, 116, 9963−9970

water−monomer bridging contacts, $\langle N_B \rangle$, which quantifies the extent to which water intrudes between hydrophobic contacts. Oligomer structure is further quantified in terms of the numbers of each distinguishable rotational conformation, trans, gauche+ and gauche−, denoted by $\langle N_t \rangle$, $\langle N_{g+} \rangle$, and $\langle N_{g-} \rangle$, respectively. We note that a rotational state is defined per every three bonds (or, equivalently, every four monomers). Consequently, a decamer has seven rotational conformations: $\langle N_t \rangle + \langle N_{g+} \rangle + \langle N_{g-} \rangle = 7$. Further, we quantified the extent of helicity by computing the number of helical contacts, $\langle N_C \rangle$, formed when all residues from i to $i + 4$ are in a gauche− state.

Changes in the oligomer configuration are a reflection of underlying fluctuations in the solvent HB network and oligomer energetics,[26] which are, themselves, reflected in the temperature dependence of the heat capacity. We therefore computed the total isochoric heat capacity of the system (C_v) using the standard thermodynamic relation

$$C_v = \frac{\langle E^2 \rangle - \langle E \rangle^2}{k_B T^2} \tag{7}$$

where E is the total potential energy of the system.

4. RESULTS

We begin by characterizing the temperature dependence of the oligomer radius of gyration, $\langle R_g \rangle$, and the number of hydration layer water molecules, $\langle N_{Hyd} \rangle$ (Figure 1a,b). The data obtained and reported in the figures are given as a function of the reduced temperature $T^* = k_B T/\varepsilon_{HB}(6)$, where $\varepsilon_{HB}(6) = 4.54$ kcal/mol is the HB energy when there are six nearest-neighbors around a H-bonded pair.[6] Error estimates are one standard deviation, computed with the jackknife binning method.[27] We first note the existence of two distinct trends in Figure 1, depending on helical stabilization: the system with $|\varepsilon_{mm}| = 4.5$ kcal/mol shows a slight monotonic decrease in $\langle R_g \rangle$ at high temperature, while $\langle N_{Hyd} \rangle$ exhibits a parabolic dependence on T^* in the middle temperature range. On the other hand, systems with a weaker helical bias show an approximately parabolic T^* dependence in both $\langle R_g \rangle$ and $\langle N_{Hyd} \rangle$ at intermediate temperatures. For systems with $|\varepsilon_{mm}| \leq 2.0$ kcal/mol, the T^* dependence suggests the existence of three different oligomer conformational regimes: a low-temperature extended ensemble at $T^* \leq 0.1$; a set of compact conformations at moderate $T^* \approx 0.2$, where $\langle R_g \rangle$ and $\langle N_{Hyd} \rangle$ are at a minimum; and a spatially extended high-T^* ensemble of conformations. At high temperatures (roughly $T^* \geq 0.25$) both $\langle R_g \rangle$ and $\langle N_{Hyd} \rangle$ values are indicative of thermal unfolding of the oligomer. We note that at $T^* = 0.44$ the size of the thermally unfolded decamer and the number of water molecules participating in its solvation are insensitive to $|\varepsilon_{mm}|$ (up 2.0 kcal/mol helical bias). Conversely, the low-temperature behavior is clearly dependent on the value of $|\varepsilon_{mm}|$: systems with $|\varepsilon_{mm}| \geq 1.7$ kcal/mol exhibit mean conformations that are more extended than the thermally unfolded decamer, whereas systems with weaker $|\varepsilon_{mm}|$ are more compact at low T^* than at high T^*.

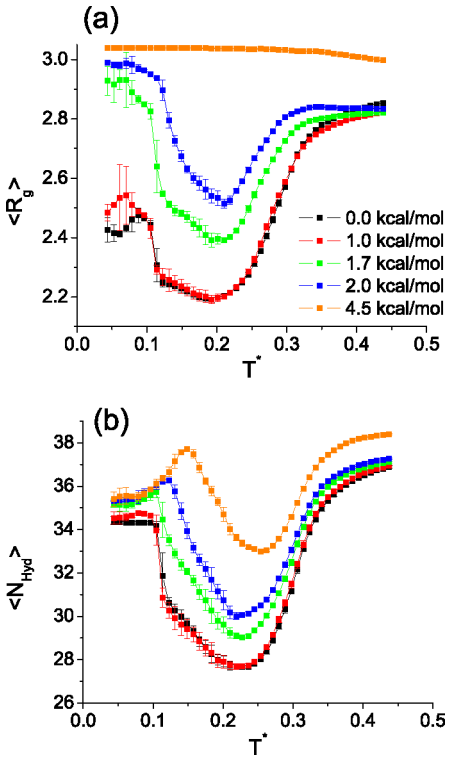

Figure 1. (a) Temperature dependence of the radius of gyration ($\langle R_g \rangle$) and (b) of the mean number of hydration-layer water molecules ($\langle N_{Hyd} \rangle$) of a solvated decamer for each indicated helical interaction energy, $|\varepsilon_{mm}|$ (see inset).

We next turn to two other structural properties—the number of helical contacts and rotational conformations—to explain the T^* dependence of $\langle R_g \rangle$ for $|\varepsilon_{mm}| = 4.5$ kcal/mol. The results are presented in Figure 2a−d. Data for $|\varepsilon_{mm}| = 4.5$ kcal/mol clearly show the existence of a stable helix up to $T^* \approx 0.2$; over this temperature range the oligomer exhibits the maximum number of helical contacts, $\langle N_C \rangle_{max} = 6$, and is composed of only gauche− rotational conformations (cf. Figures 2a and 2d for $|\varepsilon_{mm}| = 4.5$ kcal/mol). We have verified that a defect-free lattice helical decamer has $R_g = 3.04$, i.e., the value observed when $T^* \leq 0.2$ in Figure 1a. At high T^*, a slight decrease in helicity is manifested by the emergence of terminal trans and gauche+ states, at the expense of gauche− states and helical contacts. From these observations it is evident that $|\varepsilon_{mm}| = 4.5$ kcal/mol is so large that the available thermal energy is insufficient to create defects in the helix. On the contrary, as shown in Figure 1b, the hydration layer structure is T^*-dependent even if the oligomer structure is not altered. The nonmonotonicity of $\langle N_{Hyd} \rangle$ is a manifestation of hydrophobic solvation:[6] hydration-layer water molecules are stabilized by stronger HBs at low T^*; at higher temperature, however, the entropic penalty incurred by hydration molecules gains importance, leading the first layer of water to recede; hence, the minimum in $\langle N_{Hyd} \rangle$ at $T^* \approx 0.25$ (cf. Figure 1b for $|\varepsilon_{mm}| = 4.5$ kcal/mol).

Returning to systems with $|\varepsilon_{mm}| \leq 2.0$ kcal/mol, the data in Figures 2a−d also help explain the $|\varepsilon_{mm}|$ dependence of decamer structure at low temperature. The results show that the low-T^* extended oligomer conformation observed when $|\varepsilon_{mm}| = 1.7$ and 2.0 kcal/mol is due to helix formation (note in Figures 2a,d that $\langle N_C \rangle > 5$ and $\langle N_{g-} \rangle > 6$ at $T^* \leq 0.1$). For these systems, the low-T^* decamer has a higher $\langle R_g \rangle$ compared to the thermally unfolded polymer due to the more linear helix structure. As the helical stabilization becomes weaker, the numbers of helical contacts and gauche− conformations decrease monotonically at fixed temperature (gauche+ and trans show a corresponding increase; cf. Figures 2b,c). Consequently, on decreasing $|\varepsilon_{mm}|$, the low-T^* polymer configuration evolves from an extended helix to a compact

dx.doi.org/10.1021/jp305134w | J. Phys. Chem. B 2012, 116, 9963−9970

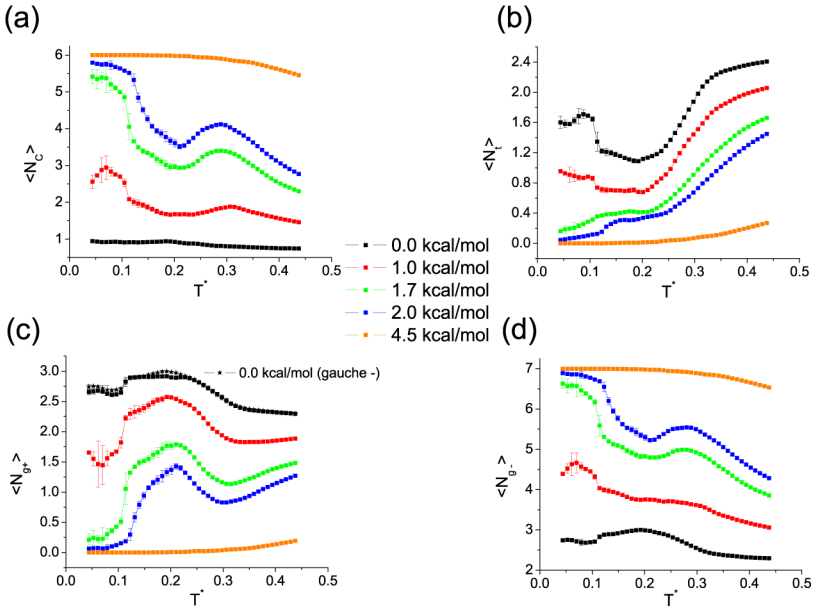

Figure 2. (a) Temperature dependence of the number of helical contacts ($\langle N_C \rangle$) of a solvated decamer for each indicated helical interaction energy (see inset). Two monomers, i and $i + 4$, form a helical contact if all residues from the ith to the $(i + 4)$th are in a gauche− rotational state. (b−d) Temperature dependence of the number of trans ($\langle N_t \rangle$), gauche+ ($\langle N_{g+} \rangle$), and gauche− ($\langle N_{g-} \rangle$) rotational states, respectively. Note the difference in vertical scales. As shown in (c), gauche+ and gauche− states occur with equal probability in the absence of helical interactions ($|\varepsilon_{mm}|$ = 0.0 kcal/mol).

globule, which explains the monotonic decrease of $\langle R_g \rangle$ with decreasing $|\varepsilon_{mm}|$ observed in Figure 1a. To further investigate the low-temperature oligomer structure when $|\varepsilon_{mm}| \leq 2.0$ kcal/mol, we computed the number $\langle N_B \rangle$ of monomer−water−monomer contacts ("water bridges"). $\langle N_B \rangle$ is defined as the number of water-mediated contacts wherein a water molecule is nearest neighbor to monomers i and $j \geq i + 3$. This property quantifies the extent to which an oligomer is solvent-penetrated, a structural feature of protein cold unfolding, inferred from NMR experiments.[28] The results are presented in Figure 3. The T^* dependence of $\langle N_B \rangle$ in Figure 3 shows that low-T^* solvent penetration is significant when $|\varepsilon_{mm}| \leq 1.0$ kcal/mol, decreasing monotonically with increasing oligomer helicity, and becoming negligible for $|\varepsilon_{mm}| \geq 2.0$ kcal/mol. This is a key observation: it suggests that the signature of cold unfolding vanishes with increasing helical bias. At higher T^*, the behavior of $\langle N_B \rangle$ shows a local minimum at $T^* \approx 0.1-0.15$ for low helical bias due to water expulsion from the hydrophobic core upon oligomer collapse. When $|\varepsilon_{mm}| \geq 1.7$ kcal/mol, on the other hand, the increase in $\langle N_B \rangle$ over this temperature range is due to helix structural degradation (note the appearance of gauche+ states in Figure 2c), which creates hydrophobic pockets. HBs within these pockets are stronger (due to $\varepsilon_{HB}^{\text{bonus}}$), driving water penetration.

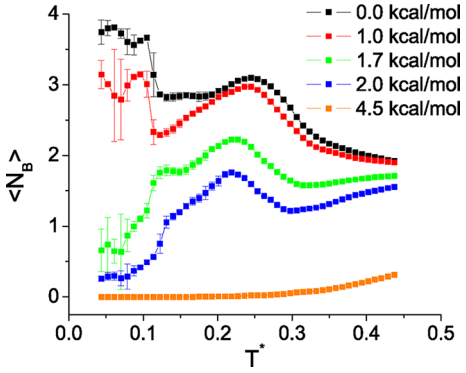

Figure 3. Temperature dependence of the number of monomer−water−monomer contacts ("water bridges", $\langle N_B \rangle$) of a solvated decamer for each indicated helical interaction energy (see inset). A molecule forms a water bridge if it is adjacent to two residues separated by three or more monomers.

Theory and computer simulations[26,31,32] have shown that polymer structural transitions are accompanied by thermodynamic signatures, such as heat capacity peaks as a function of temperature. We explore whether the conformational transitions discussed above exhibit such signatures. In Figures 4a,b we show the T^* dependence of C_v, the isochoric heat capacity per oligomer molecule. A sharp peak, associated with the low-T^* conformational transition, is observed for $|\varepsilon_{mm}| \leq 1.7$ kcal/mol at $T^* \approx 0.1$. The low-T^* peak broadens and shifts toward a higher T^* when $|\varepsilon_{mm}|$ is in the range 2.0−4.5 kcal/mol. A large, broad peak is also observed at $T^* \approx 0.3$, roughly coinciding with the onset of thermal unfolding. This peak is primarily due to the solvent. We demonstrate this by computing the solvent heat capacity from a simulation of pure water at the same fractional density (ρ_f = 0.67) as the oligomer solution. The data, presented in Figure 4c, show the existence of a large peak at $T^* \approx 0.3$. This peak is due to a sudden decrease in the number of HBs (n_{HB}) per water molecule at high T^* (Figure 4d). While the oligomer thermal denaturation is expected to manifest itself as a peak in C_v, in the systems under consideration oligomer contributions to the heat capacity are overshadowed by those of the solvent.

5. DISCUSSION

On the basis of the data of Figures 1−4 we can provide a picture as to how monomer−monomer interactions modify the conformational transitions of the solvated decamer. The discussion below focuses on systems with $|\varepsilon_{mm}| \leq 2.0$ kcal,

dx.doi.org/10.1021/jp305134w | J. Phys. Chem. B 2012, 116, 9963−9970

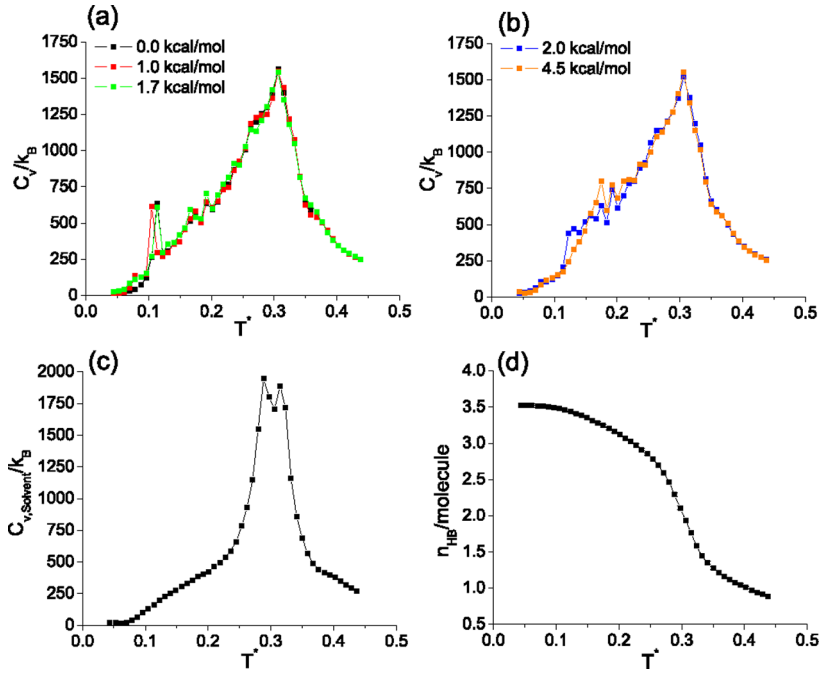

Figure 4. (a, b) Temperature dependence of the isochoric heat capacity per oligomer molecule, C_v, for each indicated helical interaction energy (see insets). (c, d) Temperature dependence of the solvent heat capacity ($C_{v,Solvent}$) and number of HBs per solvent molecule (n_{HB}), computed from a simulation of pure water at $\rho_f = 0.67$.

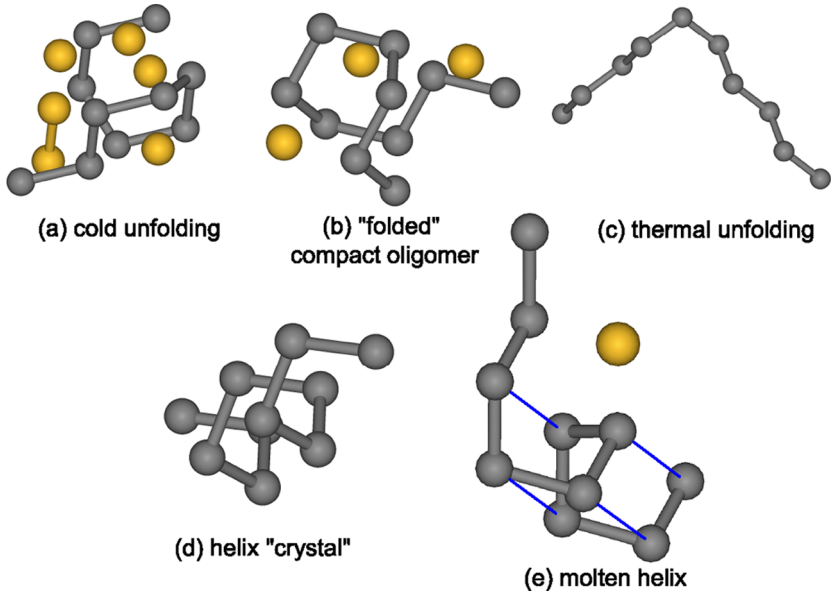

Figure 5. Renderings of representative configurations of lattice oligomers. Gray spheres and lines denote monomers and monomer−monomer covalent bonds, respectively. Yellow spheres denote water molecules involved in monomer−water−monomer contacts (water bridges). Bonds between two waters (if any) denote HBs. Parts a−c depict cold-unfolded, folded, and thermal-unfolded configurations of weakly helical decamers ($|\varepsilon_{mm}| \leq 1.0$ kcal/mol). Parts d and e show the helix and molten helix configurations observed in strongly helical systems (1.7 kcal/mol $\leq |\varepsilon_{mm}| \leq 2.0$ kcal/mol). Blue lines in part e join monomers engaged in a helical contact.

which exhibit significant chain rearrangements and hydration layer restructuring as a function of temperature. For clarity, we establish connections between structural data and representative polymer conformations, presented in Figure 5.

5.1. Weakly Helical Decamers ($|\varepsilon_{mm}| \leq 1.0$ kcal/mol). Weakly helical oligomers ($|\varepsilon_{mm}| \leq 1.0$ kcal/mol) can be described by a phase diagram similar to that of a flexible homopolymer (i.e., with no helical bias, $|\varepsilon_{mm}| = 0.0$ kcal/mol),[7] consisting of cold-unfolded conformations at low T^*, relatively dry and compact configurations at intermediate T^* ($0.1 < T^* < 0.2$), and extended, thermally unfolded conformations at high T^*. Cold-unfolding is an enthalpic process, driven by the formation of strong water−water HBs in the hydration layer;[6,7] cold-unfolded oligomers are relatively compact (in comparison with thermally unfolded oligomers) and present significant water intrusion of their hydrophobic core.[28] A representative cold-unfolded configuration is shown in Figure 5a; water molecules participating in bridges are shown in yellow. On

dx.doi.org/10.1021/jp305134w | J. Phys. Chem. B 2012, 116, 9963−9970

increasing the temperature, the decamer collapses into a more compact globular configuration with fewer water bridges, such as that presented in Figure 5b. Entropy-driven hydrophobic collapse bolsters formation of these configurations; at higher T^* the entropic penalty of hydration water becomes an important contribution to the free energy, driving the polymer to adopt a configuration that minimizes water−monomer contacts.[6,7] Further increasing T^* results in thermal unfolding, characterized by extended oligomer conformations with increasingly trans character, such as that depicted in Figure 5c.

5.2. Strongly Helical Decamers (1.7 kcal/mol ≤ $|\varepsilon_{mm}|$ ≤ 2.0 kcal/mol). For more strongly helical decamers (1.7 kcal/mol ≤ $|\varepsilon_{mm}|$ ≤ 2.0 kcal/mol), in addition to thermally unfolded configurations at high T^*, there exist two conformations whose structural features differ significantly from those of lower $|\varepsilon_{mm}|$. When $T^* \leq 0.1$, the conformation can be characterized as a "crystal", insofar as the predominant structure is that of a helical decamer with essentially no structural defects (cf. Figure 2 for 1.7 kcal/mol ≤ $|\varepsilon_{mm}|$ ≤ 2.0 kcal/mol). A representative configuration is shown in Figure 5d. Helix formation is an enthalpy-driven process;[33,34] within this range of $|\varepsilon_{mm}|$, monomer−monomer interactions are sufficiently strong to stabilize the extended helical configuration, in spite of the significant water−monomer contacts that it entails. Helical conformations show negligible water penetration, as measured by $\langle N_B \rangle$ (Figure 3 at low T^* and $|\varepsilon_{mm}| \geq 1.7$ kcal/mol). We correspondingly observe that cold unfolding vanishes with increasing helical stabilization. Heating up the crystal phase results in a transition to a more compact "molten" helix conformation. Under such conditions, the oligomer is similar to a molten globule,[35] whose structure is intermediate between that of the well-formed helix and the unfolded random coil. Although some structural degradation occurs, including the formation of water bridges, the molten helix retains a substantial degree of helicity, having ∼3.5 helical contacts (cf. Figure 2a for $|\varepsilon_{mm}|$ = 2.0 kcal/mol at $T^* \approx 0.2$). The loss of helicity is brought about by thermal fluctuations, causing the breakdown of monomer−monomer interactions and partial collapse of the chain. The collapse is manifested by the appearance of gauche+ rotational states (note the increase from 0 to ∼1 in such states at $T^* = 0.15$ when $|\varepsilon_{mm}|$ = 2.0 kcal/mol; cf. Figure 2c). A representative molten helix configuration is shown in Figure 5e, where blue lines denote helical ("i−i + 4") contacts. At $T^* > 0.3$, the molten globule undergoes thermal unfolding. The moderate increase in $\langle N_C \rangle$ and $\langle N_{g-} \rangle$ observed in the range $0.2 < T^* < 0.3$ (cf. Figures 2a,d for $|\varepsilon_{mm}|$ = 1.7 and 2.0 kcal/mol) suggests that a weakly helical intermediate[29,30] is involved in the molten globule thermal unfolding transition. The overall behavior observed in strongly helical decamers is similar to that previously reported for an isolated, flexible square-well homopolymer,[31] a system which exhibits a "solid−liquid-like" transition at low temperature between a "crystal" and a disordered globule, and a "liquid−gas-like" transition leading to an unfolded random coil.

6. SUMMARY AND CONCLUSIONS

In this paper we have described the effect of intermonomer energetics on temperature-driven conformational transitions of a hydrophobic decamer. By biasing the energetics toward gauche− states, we have focused on those interactions leading to the formation of a helical secondary structure. The monomer interaction strength, $|\varepsilon_{mm}|$, is varied over a broad range, allowing us to uncover two limiting thermodynamic scenarios. We find that when $|\varepsilon_{mm}| \leq 1.0$ kcal/mol, the hydrophobic oligomer exhibits a phase diagram characterized by cold-unfolded conformations at low temperature that are significantly water penetrated (as observed from the number of water "bridges"); more compact and dry conformations exist when $0.1 < T^* < 0.2$, and a thermally unfolded ensemble of random coils results at high temperature. On increasing $|\varepsilon_{mm}|$ to 2.0 kcal/mol, one encounters suppression of cold-unfolding, finding instead a "crystallization" transition to a helix, which undergoes a transition to a defective molten helix at higher temperature. The molten conformation differs from the compact conformation found at weaker $|\varepsilon_{mm}|$ in that, despite its relative compactness, it retains significant helical character (≥50% of helical contacts are preserved). For stronger monomer−monomer interactions (i.e., $|\varepsilon_{mm}|$ = 4.5 kcal/mol) we find that conformational transitions are largely suppressed, though the hydration layer exhibits some features of the T^* dependence expected from a hydrophobic interface.

The lattice model presented here demonstrates that a minimalist approach including hydrophobicity and monomer−monomer energetics suffices to describe a rich landscape of thermal behavior for helical oligomers. The results shown are relevant to the understanding of the thermodynamics of helical oligomers such as short alanine-based peptides, which show α-helix formation in aqueous solution.[33,36,37] In a broader context, this family of explicit-water 3-D lattice models[6] will permit studies of larger systems, such as β-sheets and helix bundles. Possible avenues for further study include the effect of sequence on oligomer stability. In this respect, a model comprising a two-letter residue alphabet could be formulated by distinguishing between hydrophobic and hydrophilic residues through explicit water−monomer interactions. Alternatively, the classification could be based on the effect of hydrophobic monomers on the entropy and enthalpy of hydration water molecules, as demonstrated by Patel et al.[38] An expanded residue alphabet would, in turn, open the door to directed evolution studies[38,39] to obtain, for example, sequences resulting in highly stable secondary structures.

AUTHOR INFORMATION

Corresponding Author

*E-mail: santiago.romero-vargas@yale.edu.

Present Address

⊥Department of Chemical and Environmental Engineering, Yale University, New Haven, CT 06520.

Notes

The authors declare no competing financial interest.

ACKNOWLEDGMENTS

P.G.D. and P.J.R. gratefully acknowledge the financial support of the National Science Foundation (Collaborative Research in Chemistry Grants CHE-0908265 (P.G.D.) and CHE-0910615 (P.J.R.)) and the R.A. Welch Foundation (grant F0019 to P.J.R.). The simulations presented in this article were performed on computational resources supported by the Princeton Institute for Computational Science and Engineering (PICSciE) and the Office of Information Technology's High Performance Computing Center and Visualization Laboratory at Princeton University.

REFERENCES

(1) Dill, K. A. *Biochemistry* **1990**, *29* (31), 7133−7155.

(2) Kauzmann, W. *Adv. Protein Chem.* **1959**, *14*, 1−63.
(3) Kauzmann, W. *Nature* **1987**, *325* (6107), 763−764.
(4) Baldwin, R. L. *Proc. Natl. Acad. Sci. U. S. A.* **1986**, *83* (21), 8069−8072.
(5) Patel, B. A.; Debenedetti, P. G.; Stillinger, F. H.; Rossky, P. J. *Biophys. J.* **2007**, *93* (12), 4116−4127.
(6) Matysiak, S.; Debenedetti, P. G.; Rossky, P. J. *J. Phys. Chem. B* **2012**, DOI: 10.1021/jp3039175.
(7) Romero-Vargas Castrillón, S.; Matysiak, S.; Stillinger, F. H.; Rossky, P. J.; Debenedetti, P. G. *J. Phys. Chem. B* **2012**, DOI: 10.1021/jp3039237.
(8) Doig, A. J. In *RSC Biomolecular Sciences*; Muñoz, V., Ed.; Royal Society of Chemistry: London, 2008; pp 1−27.
(9) Sikorski, A.; Skolnick, J. *Biopolymers* **1989**, *28* (6), 1097−1113.
(10) Sikorski, A.; Skolnick, J. *Proc. Natl. Acad. Sci. U. S. A.* **1989**, *86* (8), 2668−2672.
(11) We note that a bcc lattice can also be obtained from two interpenetrating cubic lattices.
(12) Roberts, C. J.; Debenedetti, P. G. *J. Chem. Phys.* **1996**, *105* (2), 658−672.
(13) Matysiak, S.; Debenedetti, P. G.; Rossky, P. J. *J. Phys. Chem. B* **2011**, *115* (49), 14859−14865.
(14) Poole, P. H.; Sciortino, F.; Grande, T.; Stanley, H. E.; Angell, C. A. *Phys. Rev. Lett.* **1994**, *73* (12), 1632−1635.
(15) Stillinger, F. H. *Science* **1980**, *209* (4455), 451−457.
(16) Zichi, D. A.; Rossky, P. J. *J. Chem. Phys.* **1985**, *83* (2), 797−808.
(17) Rezus, Y. L. A.; Bakker, H. J. *Phys. Rev. Lett.* **2007**, *99* (14), 148301.
(18) Bowron, D. T.; Filipponi, A.; Roberts, M. A.; Finney, J. L. *Phys. Rev. Lett.* **1998**, *81* (19), 4164−4167.
(19) Laage, D.; Stirnemann, G.; Hynes, J. T. *J. Phys. Chem. B* **2009**, *113* (8), 2428−2435.
(20) Rossky, P. J.; Zichi, D. A. *Faraday Symp. Chem. Soc.* **1982**, *17*, 69−78.
(21) Kolinski, A.; Skolnick, J.; Yaris, R. *Biopolymers* **1987**, *26* (6), 937−962.
(22) Richardson, J. S., Richardson, D. C. Principles and Patterns of Protein Conformation. *Prediction of Protein Structure and the Principles of Protein Conformation*; Plenum: New York, 1989.
(23) Wang, F. G.; Landau, D. P. *Phys. Rev. Lett.* **2001**, *86* (10), 2050−2053.
(24) Wang, F. G.; Landau, D. P. *Phys. Rev. E* **2001**, *64* (5), 056101.
(25) Challa, M. S. S.; Landau, D. P.; Binder, K. *Phys. Rev. B* **1986**, *34* (3), 1841−1852.
(26) Sharma, S.; Kumar, S. K. *J. Chem. Phys.* **2008**, *129* (13), 134901.
(27) Weigel, M.; Janke, W. *Phys. Rev. E* **2010**, *81* (6), 066701.
(28) Davidovic, M.; Mattea, C.; Qvist, J.; Halle, B. *J. Am. Chem. Soc.* **2009**, *131* (3), 1025−1036.
(29) Chikenji, G.; Kikuchi, M. *Proc. Natl. Acad. Sci. U. S. A.* **2000**, *97* (26), 14273−14277.
(30) Hamada, D.; Goto, Y. *J. Mol. Biol.* **1997**, *269* (4), 479−487.
(31) Zhou, Y. Q.; Hall, C. K.; Karplus, M. *Phys. Rev. Lett.* **1996**, *77* (13), 2822−2825.
(32) Fukugita, M.; Lancaster, D.; Mitchard, M. G. *Proc. Natl. Acad. Sci. U. S. A.* **1993**, *90* (13), 6365−6368.
(33) Marqusee, S.; Robbins, V. H.; Baldwin, R. L. *Proc. Natl. Acad. Sci. U. S. A.* **1989**, *86* (14), 5286−5290.
(34) Ooi, T.; Oobatake, M. *Proc. Natl. Acad. Sci. U. S. A.* **1991**, *88* (7), 2859−2863.
(35) Ptitsyn, O. B. *Adv. Protein Chem.* **1995**, *47*, 83−229.
(36) Mortenson, P. N.; Evans, D. A.; Wales, D. J. *J. Chem. Phys.* **2002**, *117* (3), 1363−1376.
(37) Tribello, G. A.; Ceriotti, M.; Parrinello, M. *Proc. Natl. Acad. Sci. U. S. A.* **2010**, *107* (41), 17509−17514.
(38) Patel, B. A.; Debenedetti, P. G.; Stillinger, F. H.; Rossky, P. J. *J. Chem. Phys.* **2008**, *128* (17), 175102.
(39) Arnold, F. H. *Acc. Chem. Res.* **1998**, *31* (3), 125−131.